SH53B-4221

Waves and Magnetism in the Solar Atmosphere (WAMIS)

SH53B-4221

Y.-K. Ko[1], F. Auchere[2], R. Casini[3], S. Fineschi[4], S. Gibson[3], M. Knoelker[3], C. Korendyke[1], J. M. Laming[1], S. Mcintosh[3], J. D. Moses[1], M. Romoli[5], J. Rybak[6], D. Socker[1], L. Strachan[1,7], S. Tomczyk[3], A. Vourlidas[1,8], Q. Wu[3]

[1]Naval Research Laboratory, [2]Institut d'Astrophysique Spatiale, [3]High Altitude Observatory, [4]INAF-Astrophysical Observatory of Turin, [5]University of Florence, [6]Astronomical Institute of the Slovak, Academy of Sciences, [7]also Smithsonian Research Associate, [8]now at Johns Hopkins Univ./Applied Physics Lab

1. What is WAMIS?

WAMIS is the **W**aves **A**nd **M**agnetism **I**n the **S**olar Atmosphere mission proposed for the NASA Low Cost Access to Space program. It is designed to make direct solar coronal measurements of not only the strength and orientation of the magnetic field but also the signatures of wave motions in order to better understand coronal structure, solar activity and the role of MHD waves in heating and accelerating the solar wind.

WAMIS will take advantage of greatly improved infrared (InGaAs) detectors, forward models, advanced diagnostic tools and inversion codes to obtain a breakthrough in the measurement of coronal magnetic fields and in the understanding of the interaction of these fields with space plasmas. This will be achieved with a high-altitude long-duration balloon-borne payload consisting of a coronagraph with an IR spectro-polarimeter focal plane assembly. The balloon platform provides minimum atmospheric absorption and scattering at the IR wavelengths in which these observations are made.

2. Science Objectives

I. ***What determines the magnetic structure of the corona?***
- Global structure of the coronal magnetic field
- Evolution and interaction between closed and open field regions
- Distinction between fast and slow solar wind via propagating wave properties

II. ***How do flux ropes form and evolve, and how are they related to CMEs?***
- Relationship between coronal loops, flux rope formation and CME eruption
- Magnetic structure and physical properties in prominence and prominence cavity

III. ***Where do CME-associated shocks form?***
- Observing shock formation in action in relation to the ambient coronal properties
- Measurements of shock strength, shock obliquity, and associated waves

IV. ***How is energy stored and released by reconnection in flares and CMEs?***
- Measurement of non-potential magnetic field and calculation of magnetic free energy
- Formation and properties of post-CME current sheet during CME eruption

Science Obj. I: Coronal Magnetic Structure

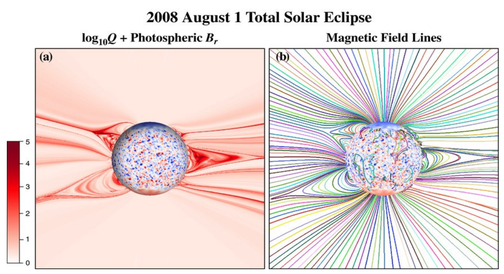

(a) Plot of squashing factor Q on logarithmic scale for the 2008 August 1 total solar eclipse. Q ~ (gradient of magnetic connectivity)^2 and high Q indicates a quasi-separatrix layer (Q -> ∞ indicates a true separatrix). (b) Magnetic field lines showing open and closed field, various field line expansions and streamer/pseudostreamer structures. Figure is from Antiochos et al. (2011).

Science Obj. II: Flux Ropes and CMEs

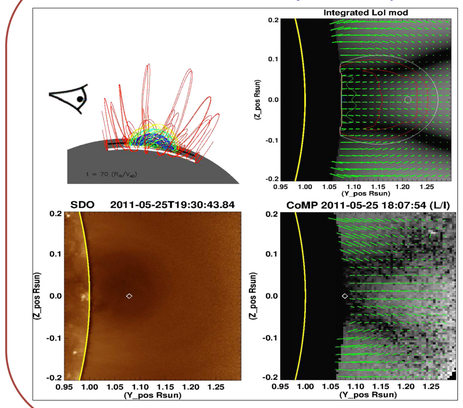

Coronal prominence cavities, e.g., as observed by SDO/AIA 193Å channel (lower left) , are often observed by CoMP to have a characteristic Fe XIII linear polarization signature (lower right; the white diamonds show the center of the cavity). This signature can be explained as arising from an arched magnetic flux rope with axis oriented along the line of sight (e.g., shown here from 3D simulation of Fan (2010); upper left). When integrated along the line of sight, a combination of linear polarization nulls, occurring where the flux rope magnetic field is oriented at the van Vleck angle θ, (cos^{2}θ=1/3), or where the axial magnetic field is oriented completely out of the plane-of-sky, leads to a forward-modeled signal of the same characteristic shape as observed (upper right; the contours show the current density in the simulations). Figure is from Bak-Steślicka et al. (2013).

Sci. Obj. III: CME Shock Formation

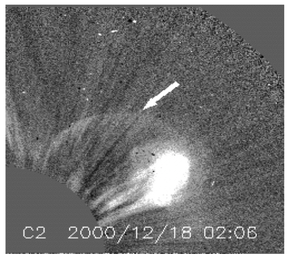

A possible example of a CME shock signature in SOHO/LASCO C2 white light observations on Dec.18, 2000. The white-light structure indicated by the arrow could be the density enhancement from a shock. A pre-event image has been subtracted from this exposure. From Vourlidas et al. (2003).

Science Obj. IV: Global Magnetic Energy Storage and Post-CME Current Sheet

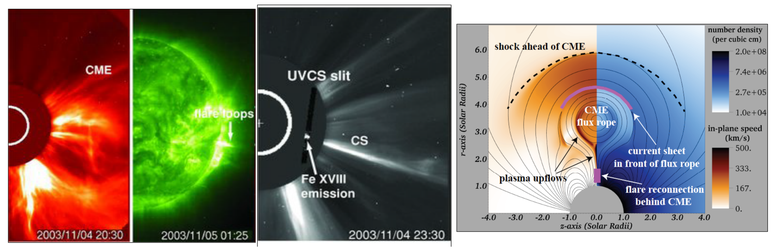

A CME with trailing post-CME current sheet. Images (left to right) are from 1) SOHO/LASCO C2 showing the CME eruption, 2) SOHO/EIT λ195 showing the post-flare loops, 3) SOHO/UVCS (the slit image of Fe XVIII λ974) and LASCO C2 (the ray-like structure) showing the post-CME current sheet. Figure is from Ciaravella & Raymond (2008). Fourth image is a simulation of breakout CME (courtesy V. Lukin). This shows the relationship between the erupting CME, the post-flare loops, and the post-CME current sheet.

3. Mission Concept Overview

Table 1. **WAMIS Long Duration Balloon (LDB) Instrument Characteristics**

Telescope type	Internally occulted Lyot coronagraph
Objective lens	f/10 singlet, aperture 20cm, focal length 203.3cm
Objective Stray Light	<0.2 $\mu B_\odot$ goal 1.2-2.8 $R_\odot$
Overall Throughput	≈5%
$B_\odot$	9.34x10^6 erg/cm^2/s/sr/nm
Plate Scale	4.5"/pixel low mag. 1.5"/pixel high mag.
Fe XIII (1074.7nm) Count Rate @ 1.1 $R_\odot$	1x10^5 photons/pixel/sec @1.5"/pixel magnification
Detector	Goodrich camera 15 micron pixels, 1280x1024 format
Inner FOV Limit	1.02 $R_\odot$
Outer FOV	±2.8 $R_\odot$ @4.5"/pixel Sun Centered
	1.8 $R_\odot$ @1.5"/pixel Limb Centered
Primary Lines of Interest	Fe XIII (1074.7, 1079.8 nm) Fe X (637.5 nm) He I (1083.0 nm)
Filter	Tunable Lyot filter, 3.8cm aperture 530 – 1083 nm range
Duration of Continuous Observational Sequence	2 weeks minimum ≥4 week optimum

Why a long duration balloon payload?

- To remove the polarization noise (variability) introduced by the Earth atmosphere
- To improve the stray light levels, hence the magnetic field measurement sensitivity by reducing the sky brightness background
- To increase the flight duration to at least 2 weeks (1/2 solar rotation) of observations without day-night cycle or weather related interruptions. This provides better temporal resolution and increases the probability for observing transients. In addition, this allows for tomographic reconstruction to separate the 3D structure of the corona from short-term temporal evolution.

4. Observational Parameters

Observational Requirements

Table 2. **Science Traceability;** see text for details

Science Objective	FoV/Spatial Resolution	Physical Observable
1.Fast/Slow Wind, Coronal B structure	1.02-1.8 $R_\odot$/1.5" pix. 1.02-2.8 $R_\odot$/4.5" pix.	Waves: Doppler velocity, B-field direction, plasma density
2. Prominences, flux ropes	1.02-1.8 $R_\odot$/1.5" pix	B-field magnitude & direction from He I and Fe XIII
3. CME Shocks	1.02-2.8 $R_\odot$/4.5" pix.	B-field magnitude & direction, plasma density; Waves: Doppler velocity,
4. Reconnection	1.02-1.8 $R_\odot$/1.5" pix.	B-field magnitude & direction, Waves: Doppler velocity, plasma density

Key Observables

Table 3. **Key WAMIS Observables**

Observable	Method of Analysis	Physical Process
Line-of-Sight B Field Strength	Circular Polarization	Long. Zeeman Effect
Plane-of-Sky B Field Direction	Linear Polarization	Resonance Scattering Effect (Hanlé)
Line-of-Sight Velocity	Intensity vs. Wavelength	Doppler Effect
Plasma Density	Fe XIII 1074.7nm/1079.8nm Intensity Ratio, K-corona from continuum	Atomic Physics, Radiation Transfer

5. Instrument Design has Strong Heritage from CoMP

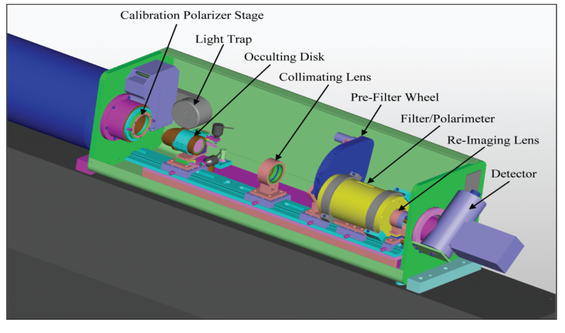

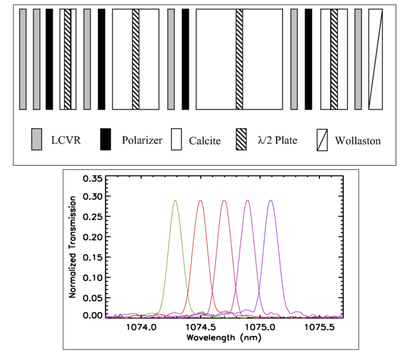

Left: A diagram showing the components of the existing Coronal Multi-channel Polarimeter (CoMP) currently operating at MLSO.
Top right: CoMP filter/polarimeter optical design. For WAMIS, the LCVRs will be replaced by FLCs, and the Wollaston beam splitter (for line and continuum outputs) is not needed.
Bottom right: Transmission profiles for 5 tunings of CoMP near the Fe XIII 1074.7 nm line.

6. Design Improvements beyond CoMP

- CoMP-S filter/polarimeter design and the Vis-IR detector will have **wider wavelength range** covering multiple ionization stages, enabling diagnostics at a range of temperatures required for both the fast and slow solar wind, as well as prominences.
- **Ferroelectric Liquid Crystals** (FLCs) will have a faster response time than the current Liquid Crystal Variable Retarders (LCVRs) on CoMP.
- Reduced atmospheric variations means that a beam splitter is not needed (spectral lines can be acquired with **higher spatial resolution**).
- f# can be optimized with **minimum instrumental polarization effect**.

7. WAMIS Coronagraph

Table 4. Optical Design

Objective	203.3cm fl.
Field Lens	31.0cm fl.
Collimating Lens	38.0cm fl.
Re-imaging Lens	High Mag. 38.0cm fl.
	Low Mag. 12.9cm fl.

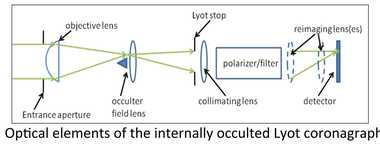

Optical elements of the internally occulted Lyot coronagraph

8. WAMIS Detector System

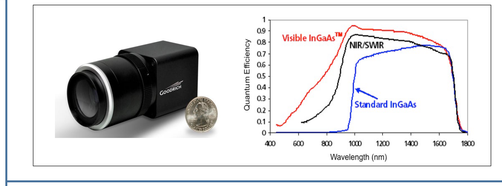

Left: Goodrich GA1280J InGaAs High Resolution Visible+SWIR camera.

Right: Detector quantum efficiency (red curve).

9. WFF WASP Gondola

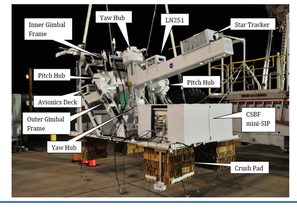

(Left) Second test flight configuration of the Wallops Arc Second Pointer (WASP) with 5m long, 450kg mock instrument.

10. WASP Gondola Pointing Performance

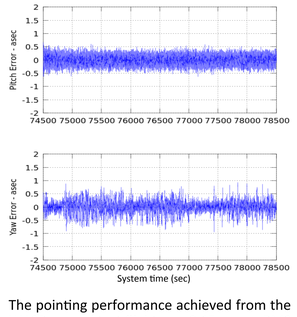

The pointing performance achieved from the WASP second test flight was 0.15 arcsec RMS pitch error (top) and 0.22 arcsec RMS yaw error (bottom).

11. Magnetic Field Measurement Sensitivity

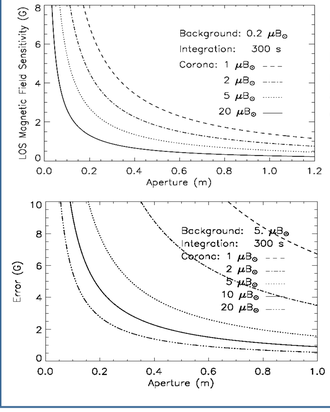

LOS B-field sensitivity in the Fe XIII line vs. aperture for different coronal intensities ($B_\odot$: mean disk brightness). **WAMIS can achieve a 2G sensitivity** in 5 min for a coronal brightness of 10$\mu B_\odot$ with a 20 cm aperture. A background (instrument stray light level) of 0.2$\mu B_\odot$ is assumed. (top panel)

On the contrary, on the ground where typical background stray light levels are higher (e.g., 5$\mu B_\odot$ for CoMP at MLSO), a 20 cm instrument would have a sensitivity of only 4.5 G. It would take 5x longer to achieve a 2 G sensitivity on the ground. (bottom panel)

Note: Wave observations (unpolarized) do not need the same accumulated exposure time for a given S/N so an image cadence as short as 2 seconds can be achieved during the post-flight analysis of the same observing programs used for the magnetic field measurements.